Effect of N-terminal region of nuclear *Drosophila melanogaster* small heat shock protein DmHsp27 on function and quaternary structure

Mohamed Taha Moutaoufik[1], Geneviève Morrow[1], Stéphanie Finet[2], Robert M. Tanguay[1]*

1 Laboratoire de génétique cellulaire et développementale, Département de biologie moléculaire, biochimie médicale et pathologie, Institut de biologie intégrative et des systèmes (IBIS) and PROTEO, Université Laval, Québec, Canada, **2** IMPMC UMR7590, CNRS, UPMC Paris 6, 4 place Jussieu, Paris, France

* Robert.tanguay@fmed.ulaval.ca

Abstract

The importance of the N-terminal region (NTR) in the oligomerization and chaperone-like activity of the *Drosophila melanogaster* small nuclear heat shock protein DmHsp27 was investigated by mutagenesis using size exclusion chromatography and native gel electrophoresis. Mutation of two sites of phosphorylation in the N-terminal region, S58 and S75, did not affect the oligomerization equilibrium or the intracellular localization of DmHsp27 when transfected into mammalian cells. Deletion or mutation of specific residues within the NTR region delineated a motif (FGFG) important for the oligomeric structure and chaperone-like activity of this sHsp. While deletion of the full N-terminal region, resulted in total loss of chaperone-like activity, removal of the (FGFG) at position 29 to 32 or single mutation of F29A/Y, G30R and G32R enhanced oligomerization and chaperoning capacity under non-heat shock conditions in the insulin assay suggesting the importance of this site for chaperone activity. Unlike mammalian sHsps DmHsp27 heat activation leads to enhanced association of oligomers to form large structures of approximately 1100 kDa. A new mechanism of thermal activation for DmHsp27 is presented.

Introduction

The small heat shock proteins (sHsps) are a ubiquitous family of ATP-independent stress proteins found in all domains of life [1–5]. They are up-regulated in response to a variety of stresses that negatively impact protein homeostasis. sHsps have a low molecular weight in the range of 12–43 kDa and are able to form large oligomeric complexes with very dynamic quaternary structure [6–10].

Small Hsps contain a tripartite architecture composed of a conserved α-crystallin domain (ACD) flanked by variable N-terminal region (NTR) and C-terminal extension (CTE) [11–13]. The NTR is highly variable in length and composition and has been partially modeled; it does not show continuous electron density suggesting a certain level of structural disorder

[6–8, 14, 15]. Indeed predictions suggest that the NTR contains some sequence bias common for intrinsically disordered proteins [16]. In vertebrate and plant sHsps this region has previously been described as a determinant of chaperone activity, substrate specificity and is essential for assembly of the higher order oligomers. [17–20]. The lack of sequence conservation and structure of the NTR in sHsps gives rise to the question as to whether it has a conserved functional role [21].

Phosphorylation of human sHsps has been reported to regulate their structure and function [22–27]. These sites of phosphorylation are located in the NTR suggesting that the phosphorylation primarily affects N-terminal contacts in the oligomer [20, 24]. Non-mammalian sHsps can also be phosphorylated: phosphorylated species of *Drosophila melanogaster* DmHsp27, DmHsp26, CG14207, maize Hsp22 and yeast Hsp26 have been described [28–32]. However, we ignore the phosphorylation effect of non-mammalian sHsps on their structure and activity [11].

Drosophila melanogaster Hsp27 (DmHsp27) is a nuclear-localized sHsp [33–35]. In addition to its up-regulation in response to stress, DmHsp27 also shows tissue- and stage-specific expression patterns during development [36]. We previously showed that, unlike metazoan sHsps, DmHsp27 forms two populations of large oligomers (725 and 540 kDa) that are able to prevent substrate aggregation [35]. Here we investigate the importance of the NTR in DmHsp27. We show that, unlike mammalian sHsps, phosphorylation of N-terminal serines in DmHsp27 does not affect the oligomeric state nor the intracellular localization of the protein.

In addition to phosphorylation sites, the NTR contains some sequences that are conserved. Deletion of a conserved FGFG motif (position F29 to G32) results in formation of large oligomers and an increase in chaperone-like activity at non-stress (non-activating) temperature using insulin as a chaperone assay. We further determined the effects of single point mutations within the FGFG motif on oligomeric structure and chaperone-like activity. Mutation of phenylalanine 29 to an alanine or tyrosine (F29A or F29Y) and glycine 30 or 32 to arginine (G30R or G32R) affects oligomerization and display a better chaperone-like activity than the wild-type protein in non-heat shock condition using insulin. Surprisingly, heat activation of DmHsp27 leads to enhanced association to form large size oligomers of approximately 1100 kDa suggest a new mechanism of thermal activation for DmHsp27.

Results

Effect of Serine phosphorylation on oligomeric structure and localization of DmHsp27

The NTR of vertebrate and plant sHsps has previously been described as a determinant of chaperoning activity and substrate specificity [17, 18]. At least, in vertebrate sHsps, post-translational modifications such as phosphorylation of serine residues found in the NTR are believed to affect the association/dissociation equilibrium of sHsps oligomers and lead to chaperone function activation [23, 37–39].

DmHsp27 is present in up to four isoforms according to the tissue and developmental stage [40]. It has been reported to be phosphorylated at NTR on at least two serines (S58 and S75) [30–32]. Whether serine phosphorylation affects the structure of DmHsp27 is an open issue. To study the effect of serine phosphorylation on the oligomeric structure and localization of DmHsp27, we constructed phosphomimetic and nonphosphorylatable mutants. To mimic phosphorylation serine (S) residues (S58 and/or S75) were substituted by aspartic acid (D) (S58D, S75D and S58/75D). To block phosphorylation, serine (S) residues (S58 and/or S75) were substituted by nonphosphorylatable alanine (A) (S58A, S75A and S58/75A). The migration profile of DmHsp27, phosphomimetic and nonphosphorylatable mutants on native gels

was compared. As reported previously [35], DmHsp27 forms two populations of oligomers with apparent molecular weight of 725 and 540 kDa. Phosphomimetic and nonphosphorylatable mutants showed the same populations as wild type DmHsp27 with a light shift for phosphomimetic mutants due to the negative charge of aspartic acid (D) (Fig 1A). All mutated constructs demonstrated the equivalent chaperone-like activity to the wild type protein with different substrates (Fig 1B and 1C).

It has been reported that phosphorylation of human HspB1 and HspB5 is a mechanism for nuclear localization in unstressed cells [41]. The role of post-translational modifications on the cellular localization of DmHsp27 was therefore examined by immunofluorescence after transfection in HeLa cells. As previously reported [34, 35, 42], phosphomimetic and nonphosphorylatable mutants of DmHsp27 showed a nuclear localization and association with nuclear speckles similar to the wild type protein. (Fig 1D). These results signify that unlike vertebrate/mammalian sHsps, the two sites of phosphorylation S58 and S75 do not affect the oligomerization equilibrium nor the intracellular localization of DmHsp27.

Further characterization of NTR in DmHsp27

The N-terminal region of sHsps is generally considered as being poorly conserved at the sequence level. Alignment of NTR of DmHsp27 with some human, murine, fish and *Methanococcus* sHsps shows high conservation of two residues (F29 and G30 in DmHsp27) (Fig 2A).

We next examined the effect of these conserved residues within the NTR on the oligomeric structure and localization of DmHsp27. A deletion of the first 86 amino acids of the N-Terminal region (Del_Nter), had a striking effect on the oligomeric equilibrium, which showed a wide band (from 480 to 146 kDa) and one extra band in the region of dimer (Fig 3A). This mutant failed to prevent heat-induced aggregation of luciferase (Luc) (Fig 3B), citrate synthase (CS) (Fig 3D), L-malate dehydrogenase (MDH), (Fig 3E) and DTT-induced aggregation of insulin (Fig 3C). Accordingly, the NTR of DmHsp27, as seen in other sHsps, is essential for oligomerization and chaperone activity at least for the substrates tested.

To further investigate residues that are important for the oligomeric structure and the chaperone-like activity of DmHsp27, we used blast similarity of NTR-DmHsp27. The obtained sequences all belong to insect sHsps. Alignment of these sequences helped to delineate a conserved sequence motif (FGXG) from phenylalanine 29 to glycine 32 in DmHsp27 (Fig 2B). Analysis of a deletion construct eliminating these four residues (del_FGFG) on a native gel, showed that the absence of this region affected the oligomeric equilibrium forming considerably large oligomers (Fig 3A). The same construct prevented heat aggregation of Luc, CS and MDH efficiently as DmHsp27 wild type (Fig 3B, 3D and 3E). Surprisingly, in non-heat condition when using insulin as a substrate, the del_FGFG construct was more efficient in prevention of DTT-induced aggregation of insulin than the WT protein (Fig 3C).

Dissecting the FGFG (29–32) motif

Since deletion of residues FGFG (29–32) induces formation of a large oligomer, we investigated this region more carefully using single point mutations. Specifically, we focused on F29 (present in all sequences examined) and F31 (less conserved), two residues with large side chains. Phenylalanine in both positions was mutated to an alanine, a smaller amino acid (F29A and F31A), or to an amino acid (tyrosine) that mimicked the size of the original amino acid but altered the hydrophobicity (F29Y and F31Y). The highly conserved glycines G30 and G32 were mutated to alanine (G30A and G32A) and to a positively charged larger amino acid arginine (G30R and G32R). Mutations in F31 (F31A and F31Y) (Fig 4A) or in G30 and G32 (G30A and G32A) (Fig 4B) had no effect on oligomerization as shown by the presence of two
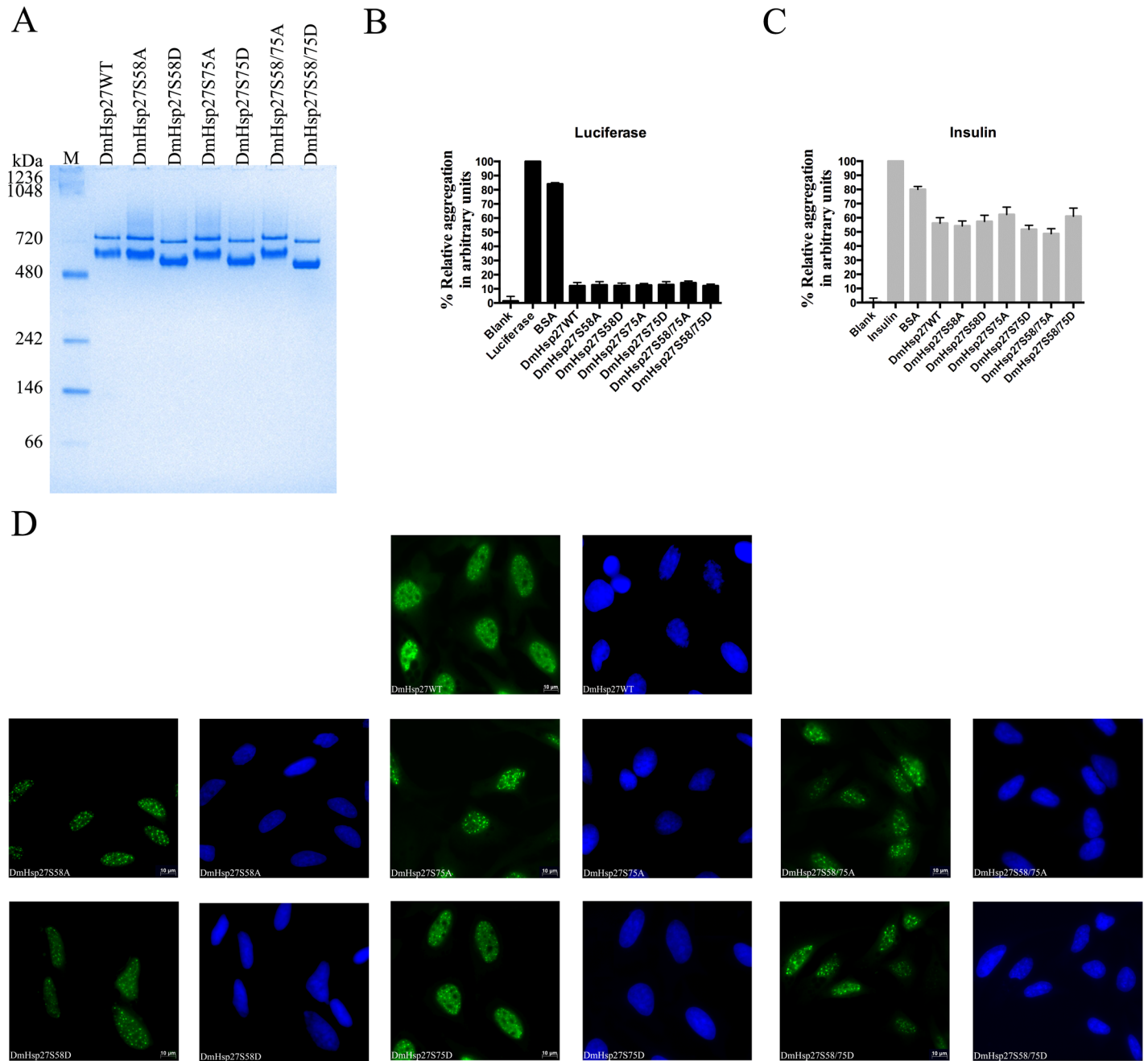
Fig 1. Phosphorylation effect on oligomerization and localization of DmHsp27. A- Native gradient (4–12%) polyacrylamide gel electrophoresis of recombinant DmHsp27 wild-type, phosphomimetic and nonphosphorylatable serine mutants. Positions of protein markers with molecular weights are shown on the left. B and C- Preventing aggregation of luciferase and insulin using phosphomimetic and nonphosphorylatable mutants. Data are representative of three independent experiments with error bars corresponding to the standard error of the mean. D- Intracellular localization of DmHSP27 and its phosphomimetic and nonphosphorylatable mutants in transfected Hela cells. Forty-eight hours post-transfection, HeLa cells were fixed, permeabilized, and processed for immunofluorescence using antibodies against DmHsp27 (green). Nuclei were counterstained with DAPI. Scale bar is 10 μm.

https://doi.org/10.1371/journal.pone.0177821.g001

bands like wild type DmHsp27. However, F29A, F29Y, G30R and G32R showed dramatic changes in oligomeric size as seen for deletion FGFG (29–32) (Fig 4A and 4B).

A
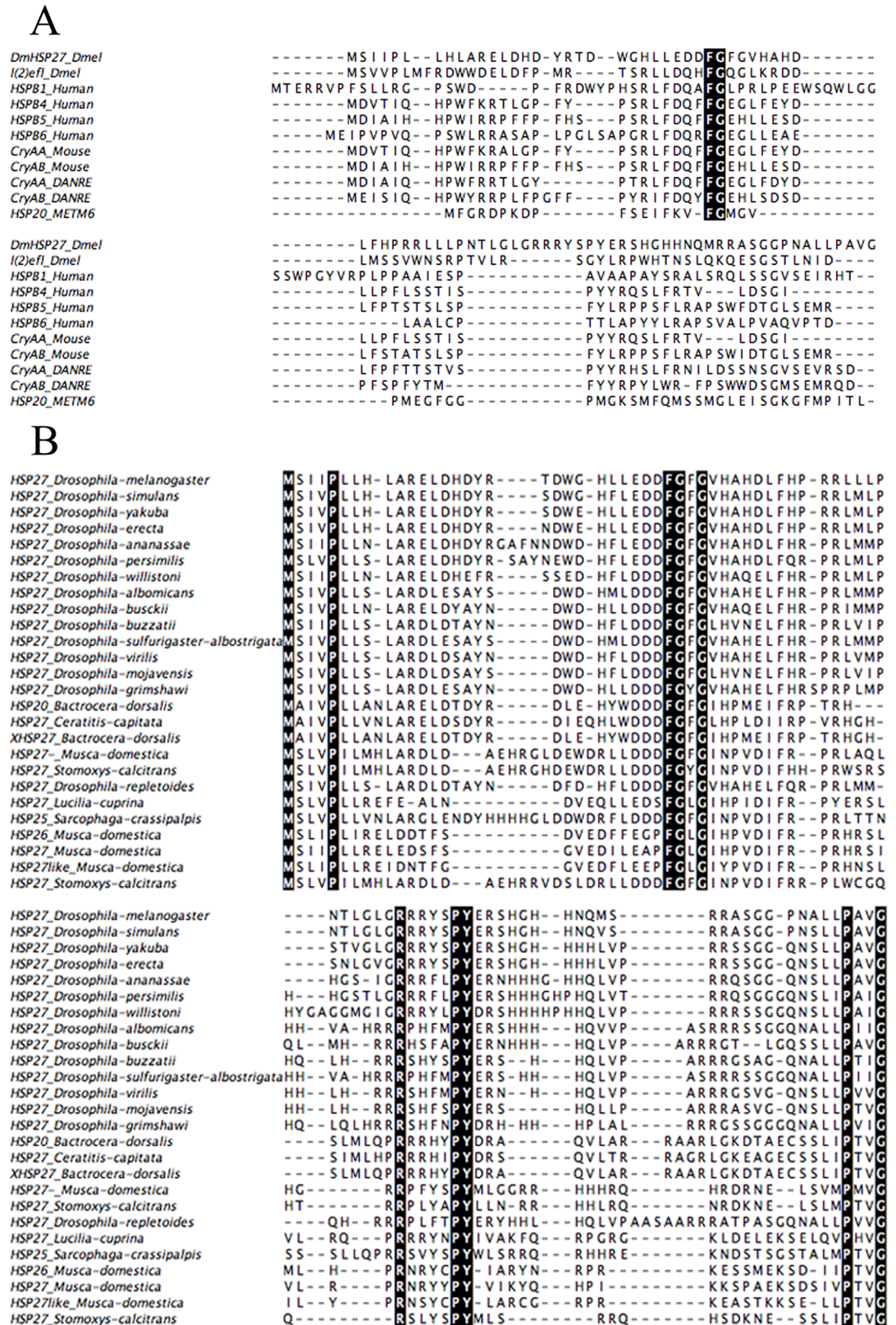

B

Fig 2. Sequence analysis of the N-terminal region of different sHsp. The alignment was made using Muscle [79]. The conserved residues are darkly highlighted in the alignment. A- Multiple sequence alignment of the NTR of DmHsp27 with I

(2)efl from *Drosophila melanogaster*, human (HspB1, HspB4, HspB5 and HspB6), Mouse (CryAA and CryAB), zebrafish (CryAA_DANRE and CryAB_DANRE) and *Methanococcus maripaludis* C6 (Hsp20_METM6). B- Multiple sequence alignment of the NTR of sHsps obtained using blast similarity of NTR-DmHsp27. Sequence from *Drosophila melqnogaster*_Hsp27, *Drosophila simulans*_Hsp27, *Drosophila yakuba*_Hsp27, *Drosophila erecta*_Hsp27, *Drosophila ananassae*_Hsp27, *Drosophila persimilis*_Hsp27, *Drosophila willistoni*_Hsp27, *Dosophila albomicans*_Hsp27, *Drosophila busckii*_Hsp27, *Drosophila buzzatii*_Hsp27, *Drosophila sulfurigaster-albostrigata*_Hsp27, *Drosophila virilis*_Hsp27, *Drosophila mojavensis*_Hsp27, *Drosophila grimshawi*_Hsp27, *Drosophila repletoides*_Hsp27, *Bactrocera dorsalis*_Hsp20, Ceratitis *capitata*_Hsp27, *Bactrocera dorsalis*_Hsp27, *Musca domestica*_Hsp27, *Stomoxys calcitrans*_Hsp27, *Lucilia cuprina*_Hsp27, *Sarcophaga crassipalpis*_Hsp25.

The size estimation by native gel electrophoresis was confirmed using SEC for DmHsp27, F29A, F29Y, G30R and G32R mutants. As seen in Fig 5, the profile of DmHsp27F29A on Superose 6 gave two peaks (Fig 5A). The first one eluted at 13 ml and corresponded to a molecular mass of 800 kDa while the second one eluted at 14.6 ml and had a molecular mass of 540 kDa. For this mutant we noted that the peak #1 corresponding to 800 kDa was more abundant than the peak #2 of 540 kDa. For DmHsp27F29Y the profile on Superose 6 shows one peak eluted at 13 ml (800 kDa) and a shoulder after the main peak at 14 ml (Fig 5B). While the R30G and R32G mutants show a single peak at 11ml corresponding to 1100 kDa (Fig 5C and 5D).
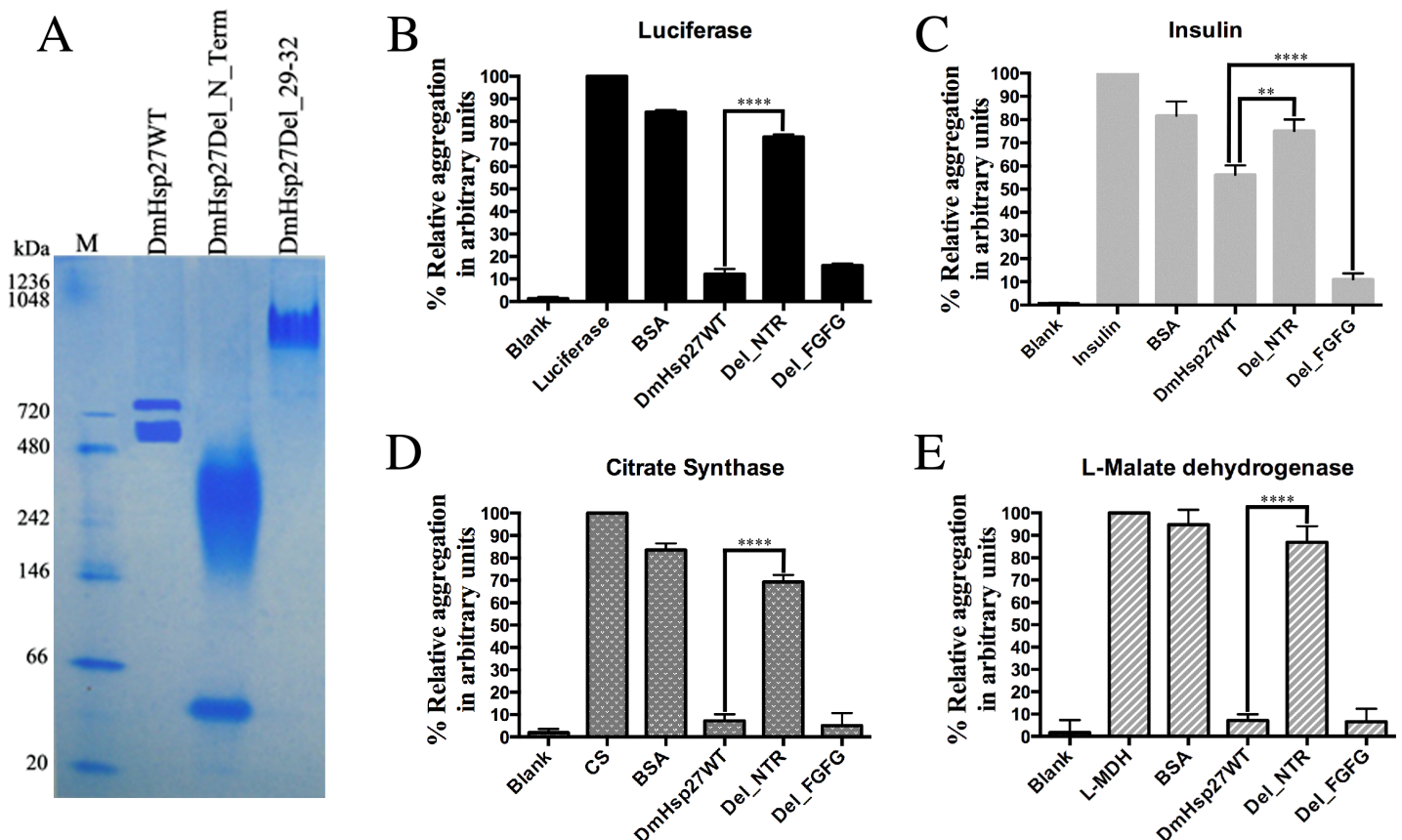
Fig 3. N-Terminal region is essential for oligomerization and chaperon-like activity. A- Native gradient (4–12%) polyacrylamide gel electrophoresis of recombinant DmHsp27 and mutants without N-terminal region and after deletion of FGFG motif at 20˚C. B, C, D and E- Prevention of aggregation of luciferase, insulin, citrate synthase and L-malate dehydrogenase using deletion of N-terminal region or deletion of 29–32 FGFG motif. The standard error calculated from 3 sets of independent experiments. ** indicates P<0.01; **** indicates P<0.0001.

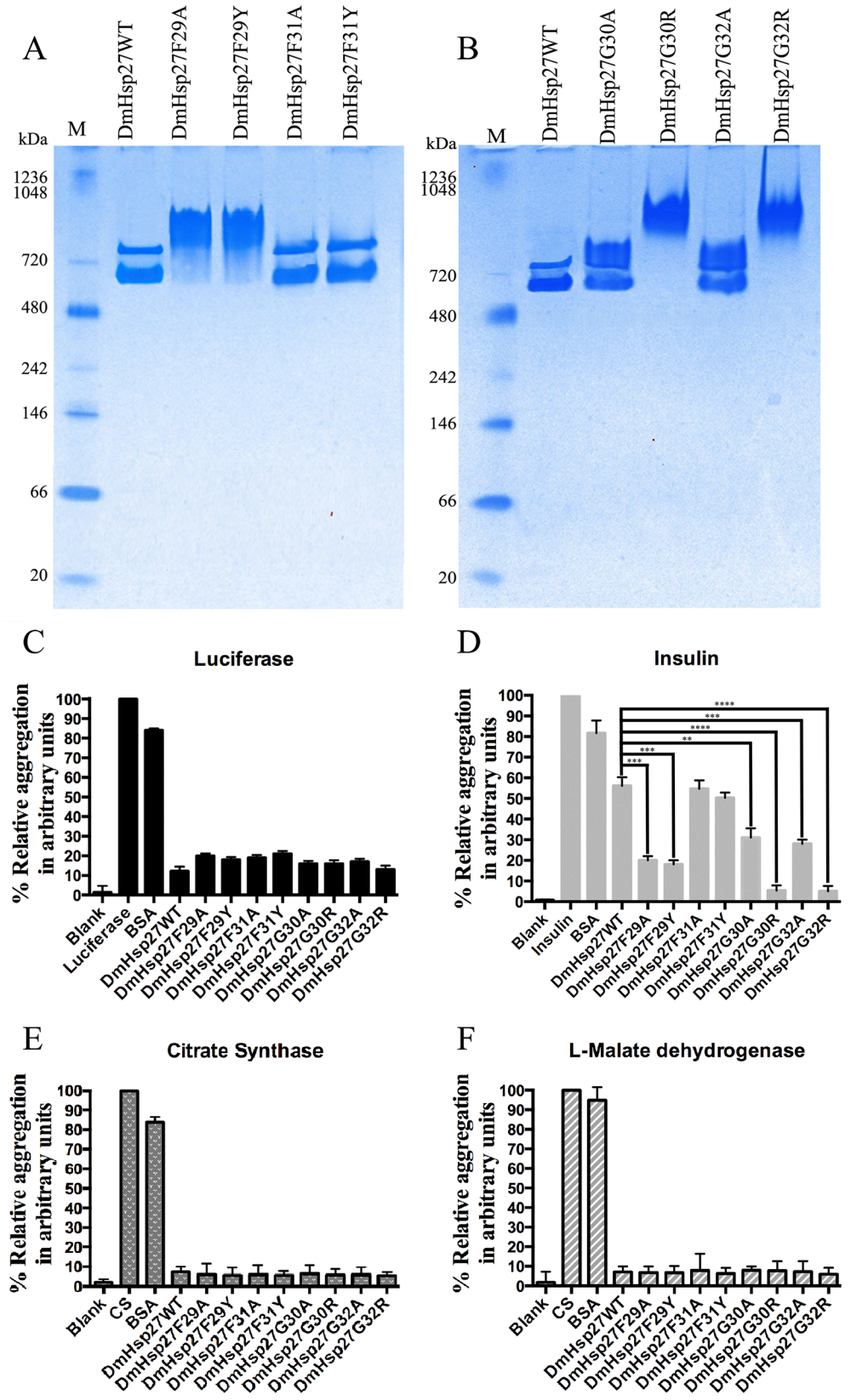**Fig 4. Effects of FGFG residues on oligomerization and chaperon-like activity.** A and B- Native gradient (4–12%) polyacrylamide gel electrophoresis of recombinant DmHsp27 and NTR mutants (F29A; F29Y, F31A, F31Y, G30A, G30R, G32A and G32R) at 20°C. Positions of standard protein markers are shown on the left. C, D, E and F- Preventing aggregation of luciferase, insulin, citrate synthase and L-malate dehydrogenase using NTR mutants (F29A; F29Y, F31A, F31Y, G30A, G30R, G32A and G32R). Data are representatives of three independent experiments. ** indicates P<0.01; *** indicates P<0.001, **** indicates P<0.0001.

Heat activation of DmHsp27

As reported previously DmHsp27WT can prevent Luc, CS, and MDH heat-induced aggregation more efficiently than insulin DTT induced aggregation [35] and Fig 4. In the same way all NTR mutants could efficiently prevent heat-induced aggregation of Luc, CS and, MDH (Fig
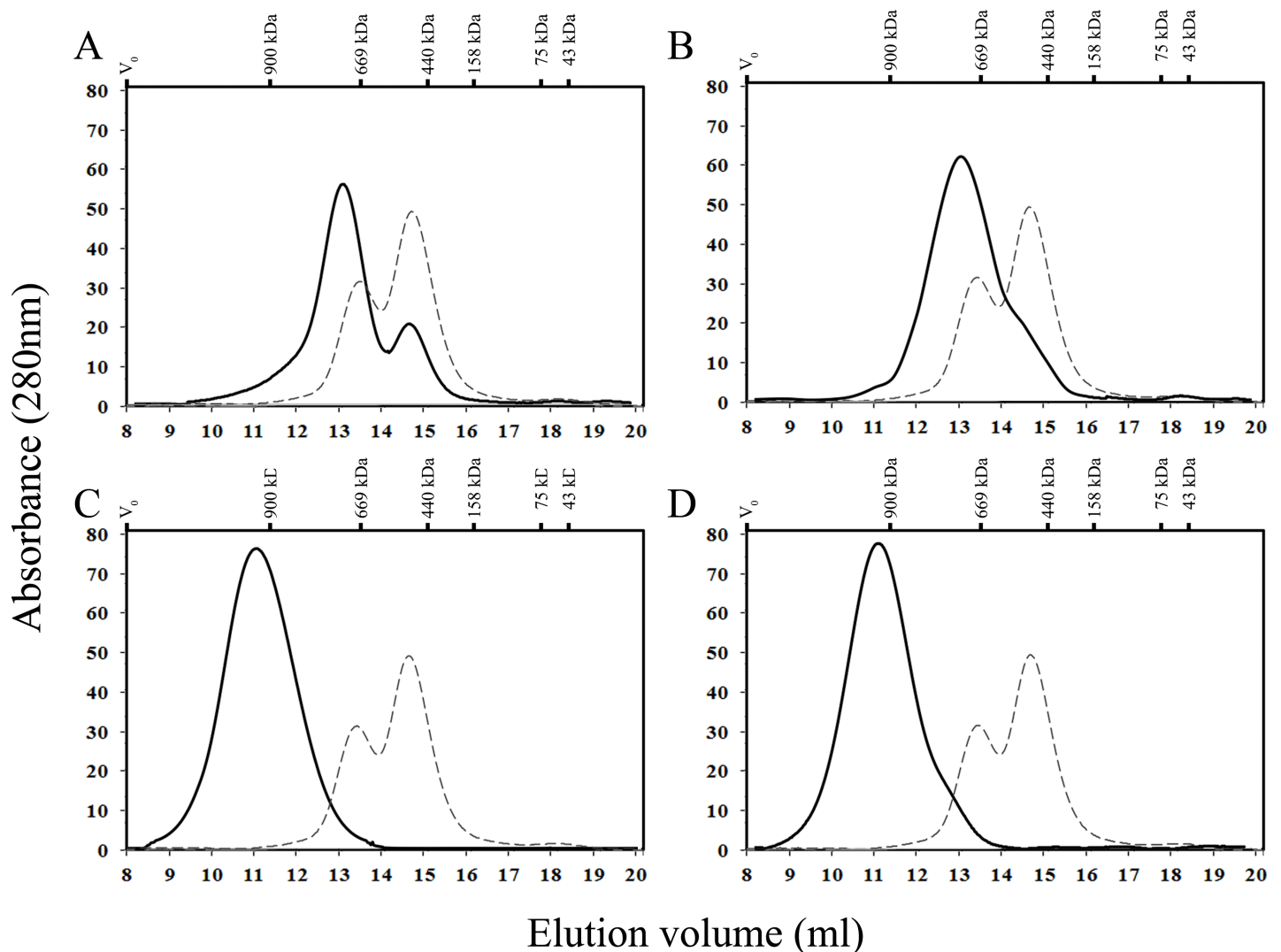
Fig 5. Size exclusion chromatography analysis of DmHsp27 N-terminal mutants F29A, F29Y, G30R and G32R. Size exclusion chromatography (SEC) analysis using a superose 6 10/300 GL (GE Life Sciences) column, with IGM (900 kDa), thyroglobulin (669 kDa), ferritin (440 kDa), aldolase (158 kDa), conalbumin (75 kDa) and ovalbumin (43 kDa) Blue dextran (2000 kDa) was used to determine the void volume of the column V_0. A- Profile on column of 300 μg (black line) of DmHsp27F29A compared to 300 μg (dashed line) of DmHsp27. B- Profile on column of 300 μg (black line) of DmHsp27F29Y compared to 300 μg (dashed line) of DmHsp27. C- Profile on column of 300 μg (black line) of DmHsp27G30R compared to 300 μg (dashed line) of DmHsp27. D- Profile on column of 300 μg (black line) of DmHsp27G32R compared to 300 μg (dashed line) of DmHsp27.

4C, 4E and 4F). No significant differences were shown in chaperone-like activity of DmHsp27 wild type and N-terminal mutants (F29A, F29Y, F31A, F31Y, G30A, G30R, G32A and G32R) in the heat-induced aggregation of Luc at 42˚C, CS and MDH at 45˚C. However, some differences in preventing aggregation using reduction of disulfide bond-induced aggregation of insulin at 20˚C were observed. DmHsp27WT, F31A and F31Y mutants were less efficient. While, mutants G30R and G32R were the most efficient followed by F29A, F29Y, G30A and G32A (Fig 4D).

It is possible that DmHsp27 binds more easily to Luc, CS and MDH than to the insulin substrate resulting in a stronger aggregation protection. Alternatively, heat activation of DmHsp27 could lead to a better protection. To test these hypotheses, we performed the insulin chaperone assay at 42˚C. DmHsp27 and all mutants showed a high capacity to reduce insulin aggregation at 42˚C compared to 20˚C (Fig 6A). At 20˚C DmHsp27WT prevented reduction-induced aggregation of insulin with 44% efficiency compared to 77.4% efficiency at 42˚C. Mutants G30A and G32A show slight improvement at 42˚C with (89.3 and 90.7% efficiency respectively) compared to 68.2 and 72.3% efficiency at 20˚C (Fig 6A). No significant difference shown for F29Y, G30R and G32R mutants. We therefore compared the oligomeric structure of DmHsp27WT and NTR mutants on a native gel at 42˚C. The results showed that at 42˚C DmHsp27WT and NTR mutants formed oligomers of higher molecular weight than those observed at 20˚C (Fig 6B and 6C). Unlike mammalian sHsps, DmHsp27 heat activation led to formation higher sized oligomers efficient to suppress aggregation of substrates.

The formation of large oligomers induced by elevated temperature are partially reversible as indicated by native gels (Supplementary S1 Fig). Interestingly, DmHsp27WT and N-terminal mutants decrease oligomeric size after recovery 30 min and 2 hours at 20˚C. It should be pointed out that for DmHsp27WT, mutants F31A, F31Y, G30A and G32A two populations of oligomers appears clearly at 2 hours recovery (S1 Fig).

Discussion

In the present work we characterized the role of a conserved motif in the NTR of DmHsp27 on its oligomeric structure and chaperone-like activity. This region is poorly conserved among sHsps and is involved in chaperoning and oligomerization.

Phosphorylation of serine residues in the NTR has been reported to regulate the chaperone activity of mammalian sHsps as recently reviewed [11, 23, 43]. A phospho-mimicking mutant of HspB1 has been found to shift the equilibrium between oligomers and dimers in favor of the smaller assemblies [39]. Similarly, studies using phosphorylation mimicking variants of HspB5 reveal an oligomer ensemble mainly consisting of 12-mers, hexamers and dimers [24]. The predominance of these smaller species indicates that the N-terminal contacts in the oligomer are influenced by phosphorylation [11]. While phosphorylation of HspB5 results in an increase in chaperone activity [24], the situation for HspB1 depends on the model substrate used [25, 37, 39, 44].

As mammalian sHsps, DmHsp27 can be phosphorylated by unknown kinase(s) on at least 2 serines in NTR (S58 and S75) [30–32]. Here we show that DmHsp27WT, and its serine 58 and 75 phosphomimetic and nonphosphorylatable mutants have the same oligomeric structure, chaperone-like activity and cellular localization. Thus unlike vertebrate/mammalian sHsps, phosphorylation of S58 and S75 in the NTR does not affect the oligomerization equilibrium nor the nuclear localization of DmHsp27.

Using molecular dynamics simulations Patel et al. [45] showed that the NTR of a sHsp dimer is flexible/dynamic and presents two major conformational forms designated "open" or "closed" suggesting that the NTR of the dimer behaves as a structural domain. Complete
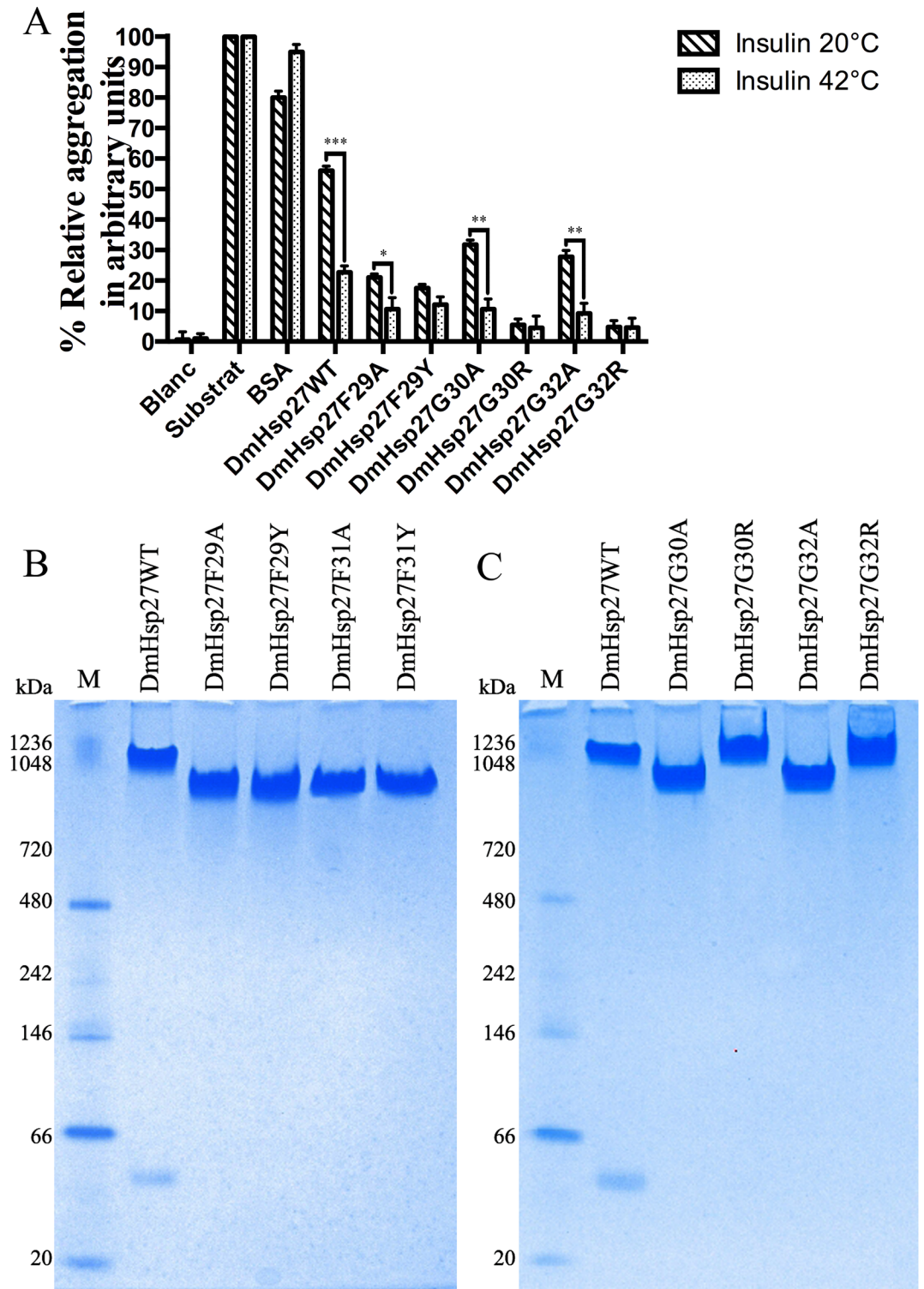
Fig 6. Study of heat activation of DmHsp27 and its FGFG mutants. A- Prevention of aggregation of insulin using DmHsp27WT and NTR mutants at 42˚C compared to 20˚C. Data are representative of three independent experiments, error bars resultant the standard error of the mean. B and C- Native gradient (4–12%) polyacrylamide gel electrophoresis of recombinant DmHsp27 and NTR mutants at 42˚C. Positions of standard protein markers with known molecular weights are shown on the left. * indicates $P<0.05$, ** indicates $P<0.01$; *** indicates $P<0.001$.

deletion of DmHsp27 N-terminal region leads to disruption of oligomerization and loss of chaperone function. Studies by incorporation of hydrophobic dyes, cross-linking experiments and analyses by mass spectrometry suggested that substrates bind to segments in the NTR [46–49]. Decreased of chaperone activity for DmHsp27_Del_N_Term is not linked to dissociation of oligomeric assembly but to binding role of NTR. As shown for many sHps removal of N-terminal in many sHsps leads to loss of chaperone function [18, 50–56], suggests a conserved role of N-terminal in oligomerization and chaperone-like activity.

Although, NTR has been described as poorly conserved, we delineate a conserved motif phenylalanine 29 to glycine 32 (FGFG) in orthologues of DmHsp27. This motif is equivalent to the described "the phenylalanine-rich region" in vertebrate sHsps [57]. A larger deletion that also eliminated this motif in human HspB4 and HspB5 resulted in a decrease of oligomeric size and an increase of chaperone-like activity [58]. In the case of DmHsp27 deletion of the conserved motif from phenylalanine 29 to glycine 32 (FGFG) affected the oligomeric state differently, with the formation of large oligomers, but resulted in enhancement of chaperone-like activity in non-thermal conditions using insulin. This suggests that there is at least one important residue that modulates oligomerization and chaperone-like activity in this region. We found that the less conserved residue F31 had no effect on quaternary structure nor the chaperone-like activity of DmHsp27. F29 seems important for formation of the smaller 540 kDa species seen by gel filtration [35], whereby mutation of this residue to either an alanine or tyrosine resulted in predominantly larger oligomers with molecular weights close to the 800 kDa species. G30R and G32R destabilized the balance to form a single peak corresponding to a higher oligomer with the highest chaperone-like activity in non-thermal conditions using the insulin assay.

Previous studies on the structure of Hsp16.9 from wheat [7] and Hsp16.0 from yeast [8] highlighted the important role of phenylalanines in the N-terminal region in oligomer formation and chaperone-like activity. Other studies using bovine or murine alphaB-crystallin, showed that mutation of F24, F27 or F28 decrease the oligomeric size and chaperone-like activity at elevated temperatures [59–61]. Recently, Heirbaut et al [18] showed that mutants of the conserved phenylalanine at position 33 to alanine in NTR of HspB6 was less active in insulin and yeast alcohol dehydrogenase aggregation assays and this residue was linked to the self-association properties of HspB6. F28 in bovine αB-crystallin and F33 in human HspB6, which are equivalent to F29 in DmHsp27 showed different behavior compared to F29 of DmHsp27. Interestingly mutation of glycine at position 34 to arginine in the NTR of HspB1 (equivalent to glycine at position 30 in DmHsp27) has been associated to distal hereditary motor neuropathies [62]. A study by Muranova et al [63] showed that mutant HspB1-G34R forms stable oligomers slightly larger than the corresponding oligomers of the HspB1WT and decreased chaperone-like activity.

There is significant controversy concerning the mode of activation of sHsps. sHsps reveal temperature-dependent chaperone activity in preventing aggregation of substrate proteins [64, 65]. Most chaperone activity models suggests that sHsps dissociate to small oligomeric forms, presumably dimers, which re-associate to a new oligomeric form containing the bound substrate [11, 12, 66–68]. However, some sHsps are activated differently. For example, the transition of Hsp26 from *Saccharomyces cerevisiae*, in which the transition into a state of increased substrate binding affinity and chaperone activity occurs through slight conformational changes without perturbation of the oligomeric state [69]. Another example is plant class II sHsps, that remain oligomeric but undergo structural rearrangements [70]. HspB1 exhibits heat-induced self-association, leading to increased oligomeric size, which correlates with increase in its chaperone-like activity [71]. Hsp22 (HspB8) from rat reveals heat-induced conformational changes with increased exposure of hydrophobic surfaces and chaperone-like

activity [72]. *C. elegans* Hsp17 forms large sheet-like super-molecular assemblies (SMA) at high temperatures and only the SMA form exhibits chaperone-like activity in suppressing the aggregation of non-native substrate proteins [73]. It is clear that not all sHsps are activated by the same mechanism. In the case of DmHsp27, we observed a partial reversible heat-activation by induced structural changes that result in formation of higher oligomers of approximately 1100 kDa. DmHsp27WT is more effective as a chaperone at 42°C than 20°C using insulin. This suggests that heat enhances DmHsp27 chaperone-like activity by formation of larger oligomers.

How heat induces oligomerization of DmHsp27 is still an open question. In general, temperature-dependent conformational change in sHsps increases exposure of hydrophobic surfaces leading to increase in the chaperone-like activity by interaction with partially unfolded proteins through hydrophobic surfaces and prevents their aggregation. Two studies with alpha-crystallin from bovine lens support this proposition. First Das et al [74] showed exposure of hydrophobic surfaces at high temperature. Second, Smith et al [75] showed that hydrophobic regions around the residues 32–37 and 72–75 of αA- and 28–34 of αB-crystallin were exposed above 30°C.

In summary, this study characterized DmHsp27 mutant in the N-terminal region and we suggest a new protection mechanism played by DmHsp27 as molecular chaperone.

Material and methods

Cloning, expression and purification of recombinant DmHsp27

The cDNA of wild type DmHsp27 (DmHsp27WT) was cloned using GIBSON ASSEMBLY (NEB) into bacterial expression vector pETHSUK (a gift from Dr. S.Weeks, [76]) and mammalian expression vector pcDNA3.1$^{(+)}$ at KpnI and XhoI sites by PCR as described in [35]. Mutations were introduced by using suitable oligomers (Table 1) and site-directed mutagenesis were done using Gibson assembly (NEB) and confirmed by DNA sequencing.

Following the detailed protocol in [35] pETHSUK DmHsp27WT and its N-terminal mutants were expressed in Escherichia coli BL21 (DE3) pLysS strain (NEB). The protein expression was induced with isopropyl-β-thiogalactoside (IPTG) (Roche).

The protein purification was accomplished by affinity chromatography using Ni-NTA agarose (Qiagen) column. His-Sumo-tag was digested with Sumo-Hydrolase followed by size exclusion chromatography (SEC) on Superose 6 10/300 column (GE Lifesciences) as described earlier [35]. All mutants gave a good yield of pure protein (25 mg/l) and could be concentrated above 15 mg/ml.

Analysis of the quaternary structure by size exclusion chromatography

SEC was used to analyze the quaternary structure of DmHsp27. 300μg of proteins were loaded on Superose 6 10/300 column (GE Lifesciences) equilibrated with 20 mM Tris-HCl pH 8, 150 mM NaCl. SEC was achieved at room temperature and eluted at 0.5 ml/min. For estimating the molecular weight, the column was calibrated with protein markers immunoglobulin M (IGM) from bovine serum (900 kDa) (Sigma), (thyroglobulin (669 kDa), Ferritin (440 kDa), Aldolase (158 kDa), Conalbumin (75 kDa), Ovalbumin (43 kDa) and Blue Dextran 2000 to determine the void volume) (GE Lifesciences) as detailed in [35].

Analysis of the quaternary structure by native gel electrophoresis

For native gel electrophoresis samples were kept at room temperature (20°C) or heated at 42°C using a water bath during 10 min and loaded on a gel 4–12% gradient native Tris-Glycine

Table 1. Primers sequences used to construct DmHsp27 NTR mutants.

Primer	Primer sequences
pETHSUK DmHsp27Fwd	5′–AGATTGGTGGTACCATGTCAATTATACCACTGC–3′
pETHSUK DmHsp27Rev	5′–AGCAGAAGCTTCTTACTTGCTAGTCTCCATTTTC–3′
pcDNA DmHsp27Fwd	5′–AAACTTAAGCTTGGTACATGTCAATTATACCACTGC–3′
pcDNA DmHsp27Rev	5′–CGGGCCCTCTAGACTTACTTGCTAGTCTCCATTTTC–3′
pETHSUK DmHsp27Del-NTRFwd	5′–GAACAGATTGGTGGTACAATGAAAGATGGCTTCCAG–3′
DmHsp27Del29-32Fwd	5'–GGAGGATGACGTCCATGCCCACGATCTGTTCC–3'
DmHsp27Del29-32Rev	5'–GGGCATGGACGTCATCCTCCAGCAAATGCCCCC–3'
DmHsp27F29AFwd	5′–GAGGATGACGCCGGTTTTGGCGTCCATGCCTAT–3′
DmHsp27F29ARev	5'–GACGCCAAAAGCGGCGTCATCCTCCAGC–3'
DmHsp27F29YFwd	5′–GAGGATGACTACGGTTTTGGCGTCCATGCCTAT–3′
DmHsp27F29YRev	5'–GACGCCAAAAGCGTAGTCATCCTCCAGC–3'
DmHsp27G30AFwd	5'–GAGGATGACTTCGCTTTTGGCGTCCATGCC–3'
DmHsp27G30ARev	5'–GAC GCC AAA AGC GAA GTC ATC CTC CAG C–3'
DmHsp27G30RFwd	5'–GAG GAT GAC TTC CGT TTT GGC GTC CAT GCC–3'
DmHsp27G30RRev	5'–GAC GCC AAA ACG GAA GTC ATC CTC CAG C–3'
DmHsp27F31AFwd	5'–GAGGATGACTTCGGTGCTGGCGTCCATGCC–3'
DmHsp27F31ARev	5'–GACGCCAGCACCGAAGTCATCCTCCAGC–3'
DmHsp27F31YFwd	5'–GAGGATGACTTCGGTTATGGCGTCCATGCC–3'
DmHsp27F31YRev	5'–GACGCCATAACCGAAGTCATCCTCCAGC–3'
DmHsp27G32A$_{Fwd}$	5'–GACTTCGGTTTTGCCGTCCATGCCCACG–3'
DmHsp27G32A$_{Rev}$	5'–GGCATGGACGGCAAAACCGAAGTCATCC–3'
DmHsp27G32R$_{wd}$	5'–GACTTCGGTTTTCGCGTCCATGCCCACG–3'
DmHsp27G32R$_{ev}$	5'–GGCATGGACGCGAAAACCGAAGTCATCC–3'
DmHsp27S58AFwd	5′–CGTCGTCGCTATGCGCCGTACGAGAGG–3′
DmHsp27S58ARev	5′–CCTCTCGTACGGCGCATAGCGACGCGACC–3′
DmHsp27S58DFwd	5′–CGTCGTCGCTATGACCCGTACGAGAGG–3′
DmHsp27S58DFwd	5′–CCTCTCGTACGGGTCATAGCGACGCGACC–3′
DmHsp27S75AFwd	5′–CACGTCGCGCGGCGGGAGGTCCAAACG3–′
DmHsp27S75ARev	5′–CGTTTGGACCTCCCGCCGCGCGACGTG–3′
DmHsp27S75DFwd	5′–CACGTCGCGCGGACGGAGGTCCAAACG3–′
DmHsp27S75DRev	5′–CGTTTGGACCTCCGTCCGCGCGACGTG–3′

Fwd: forward.

Rev: reverse.

gels (Thermo Fisher Scientific). Gels were run at 150 V at room temperature (20˚C) or at 42˚C (on a water bath) using pre-cast Mini-Cell electrophoresis system (XCell SureLock, Life Technology). The protein complexes were stained with Coomassie blue immediately after electrophoresis.

Chaperone-like activity

Luciferase, citrate synthase, L-malate dehydrogenase and insulin were used as substrates to evaluate the chaperone-like activity as as described in Morrow et al 2006 [77] and Moutaoufik et al. 2016 [35].

The heat-induced aggregation assay was performed using: luciferase (0.1 μM, Promega) at 42˚C, citrate synthase (0.16 μM; Sigma) and L-malate dehydrogenase (0.65 μM; Roche) at 45˚C in the absence or presence of DmHsp27 or its mutants. Altough, insulin (52 μM, Sigma)

non-Heat-induced aggregation was induced by disulfide bonds reduction at 20°C. All substrats were pre-incubated alone or in the presence of DmHsp27 or its mutants and aggregation was followed by an increase in the optical density at 320 nm on a spectrophotometer with thermo-stated cells.

Cell culture, transfection conditions and immunofluorescence analyses

Hela cells were maintained in MEM Alpha (Gibco) supplemented with 5% FBS. Cells were plated in advance at a confluence of 175 000 cells/well (6 well plate) containing glass coverslip for transfection. Later, cells were incubated for 4 h in OptiMEM (Gibco) containing the plasmid pcDNA3.1$^{(+)}$-DmHsp27:Lipofectamine (Invitrogen) complex (1.5 μl Lipofectamine/1.5 μg DNA), cells were washed with culture medium and incubated for 48 h to express DmHsp27 before immunofluorescence.

Immunofluorescence was performed as described in [35, 78]. Briefly, cells were washed with PBS and fixed in methanol at − 20 C for 20 min. Cells were blocked in PBS 0.1% Tween20-X (PBST) containing 5% BSA (PBST-BSA) and were incubated one hour at room temperature with primary antibody (monoclonal anti-DmHsp27 (2C8E11) [34, 35]) diluted (1/20) in PBST-BSA. After they, were washed with PBST and were incubated 45 min with secondary anti-body (goat anti-mouse Alexa 488 (Invitrogen)). Finally, cells were mounted in Vectashield mounting medium (Vector Laboratories) and examined using fluorescence microscopy (Axio Observer Z1).

Supporting information

S1 Fig. Partial reversibility after heat activation of DmHsp27 and its FGFG mutants. Native gradient (4–12%) polyacrylamide gel electrophoresis of recombinant DmHsp27 and NTR mutants heated at 42°C for 1h and cooled back at 20°C for 30 min (A) or 2h (B). Positions of standard protein markers with known molecular weights are shown on the left. (TIF)

Acknowledgments

Author Contributions

Conceptualization: MTM GM RMT.

Data curation: MTM RMT.

Formal analysis: MTM GM RMT.

Funding acquisition: SF RMT.

Investigation: MTM GM.

Methodology: MTM GM RMT.

Project administration: GM.

Resources: SF RMT.

Software: RMT.

Supervision: RMT.

Validation: MTM GM.

Visualization: MTM GM RMT.

Writing – original draft: MTM RMT.

Writing – review & editing: MTM GM SF RMT.

References

1. Maaroufi H, Tanguay RM. Analysis and phylogeny of small heat shock proteins from marine viruses and their cyanobacteria host. PLoS One. 2013; 8(11):e81207. Epub 2013/11/23. PubMed Central PMCID: PMC3827213. https://doi.org/10.1371/journal.pone.0081207 PMID: 24265841

2. Caspers GJ, Leunissen JA, de Jong WW. The expanding small heat-shock protein family, and structure predictions of the conserved "alpha-crystallin domain". J Mol Evol. 1995; 40(3):238–48. Epub 1995/03/01. PMID: 7723051

3. de Jong WW, Caspers GJ, Leunissen JA. Genealogy of the alpha-crystallin—small heat-shock protein superfamily. Int J Biol Macromol. 1998; 22(3–4):151–62. Epub 1998/07/03. PMID: 9650070

4. Fu X, Jiao W, Chang Z. Phylogenetic and biochemical studies reveal a potential evolutionary origin of small heat shock proteins of animals from bacterial class A. J Mol Evol. 2006; 62(3):257–66. Epub 2006/02/14. https://doi.org/10.1007/s00239-005-0076-5 PMID: 16474980

5. Bourrelle-Langlois M, Morrow G, Finet S, Tanguay RM. In Vitro Structural and Functional Characterization of the Small Heat Shock Proteins (sHSP) of the Cyanophage S-ShM2 and Its Host, Synechococcus sp. WH7803. PLoS One. 2016; 11(9):e0162233. PubMed Central PMCID: PMCPMC5028025. https://doi.org/10.1371/journal.pone.0162233 PMID: 27643500

6. Kim KK, Kim R, Kim SH. Crystal structure of a small heat-shock protein. Nature. 1998; 394(6693):595–9. Epub 1998/08/26. https://doi.org/10.1038/29106 PMID: 9707123

7. van Montfort RL, Basha E, Friedrich KL, Slingsby C, Vierling E. Crystal structure and assembly of a eukaryotic small heat shock protein. Nat Struct Biol. 2001; 8(12):1025–30. Epub 2001/11/10. https://doi.org/10.1038/nsb722 PMID: 11702068

8. Hanazono Y, Takeda K, Oka T, Abe T, Tomonari T, Akiyama N, et al. Nonequivalence observed for the 16-meric structure of a small heat shock protein, SpHsp16.0, from Schizosaccharomyces pombe. Structure. 2013; 21(2):220–8. Epub 2013/01/01. https://doi.org/10.1016/j.str.2012.11.015 PMID: 23273429

9. Stengel F, Baldwin AJ, Painter AJ, Jaya N, Basha E, Kay LE, et al. Quaternary dynamics and plasticity underlie small heat shock protein chaperone function. Proc Natl Acad Sci U S A. 2010; 107(5):2007–12. Epub 2010/02/06. PubMed Central PMCID: PMC2836621. https://doi.org/10.1073/pnas.0910126107 PMID: 20133845

10. Benesch JL, Aquilina JA, Baldwin AJ, Rekas A, Stengel F, Lindner RA, et al. The quaternary organization and dynamics of the molecular chaperone HSP26 are thermally regulated. Chem Biol. 2010; 17(9):1008–17. Epub 2010/09/21. PubMed Central PMCID: PMC3388541. https://doi.org/10.1016/j.chembiol.2010.06.016 PMID: 20851350

11. Haslbeck M, Vierling E. A first line of stress defense: small heat shock proteins and their function in protein homeostasis. J Mol Biol. 2015; 427(7):1537–48. Epub 2015/02/15. PubMed Central PMCID: PMC4360138. https://doi.org/10.1016/j.jmb.2015.02.002 PMID: 25681016

12. Basha E, O'Neill H, Vierling E. Small heat shock proteins and alpha-crystallins: dynamic proteins with flexible functions. Trends Biochem Sci. 2012; 37(3):106–17. Epub 2011/12/20. PubMed Central PMCID: PMC3460807. https://doi.org/10.1016/j.tibs.2011.11.005 PMID: 22177323

13. Kappe G, Boelens WC, de Jong WW. Why proteins without an alpha-crystallin domain should not be included in the human small heat shock protein family HSPB. Cell Stress Chaperones. 2010; 15(4):457–61. Epub 2009/11/19. PubMed Central PMCID: PMC3082639. https://doi.org/10.1007/s12192-009-0155-4 PMID: 19921466

14. McHaourab HS, Lin YL, Spiller BW. Crystal structure of an activated variant of small heat shock protein Hsp16.5. Biochemistry. 2012; 51(25):5105–12. Epub 2012/06/08. PubMed Central PMCID: PMC3384710. https://doi.org/10.1021/bi300525x PMID: 22670769

15. Bepperling A, Alte F, Kriehuber T, Braun N, Weinkauf S, Groll M, et al. Alternative bacterial two-component small heat shock protein systems. Proc Natl Acad Sci U S A. 2012; 109(50):20407–12. Epub 2012/11/28. PubMed Central PMCID: PMC3528540. https://doi.org/10.1073/pnas.1209565109 PMID: 23184973

16. Weeks SD, Bouckaert J. Small-angle X-ray scattering to obtain models of multivalent lectin-glycan complexes. Methods Mol Biol. 2014; 1200:511–26. https://doi.org/10.1007/978-1-4939-1292-6_42 PMID: 25117261

17. Basha E, Friedrich KL, Vierling E. The N-terminal arm of small heat shock proteins is important for both chaperone activity and substrate specificity. J Biol Chem. 2006; 281(52):39943–52. Epub 2006/11/09. https://doi.org/10.1074/jbc.M607677200 PMID: 17090542

18. Heirbaut M, Beelen S, Strelkov SV, Weeks SD. Dissecting the functional role of the N-terminal domain of the human small heat shock protein HSPB6. PLoS One. 2014; 9(8):e105892. PubMed Central PMCID: PMCPMC4144951. https://doi.org/10.1371/journal.pone.0105892 PMID: 25157403

19. Jehle S, Vollmar BS, Bardiaux B, Dove KK, Rajagopal P, Gonen T, et al. N-terminal domain of alphaB-crystallin provides a conformational switch for multimerization and structural heterogeneity. Proc Natl Acad Sci U S A. 2011; 108(16):6409–14. Epub 2011/04/06. PubMed Central PMCID: PMC3081008. https://doi.org/10.1073/pnas.1014656108 PMID: 21464278

20. Braun N, Zacharias M, Peschek J, Kastenmuller A, Zou J, Hanzlik M, et al. Multiple molecular architectures of the eye lens chaperone alphaB-crystallin elucidated by a triple hybrid approach. Proc Natl Acad Sci U S A. 2011; 108(51):20491–6. Epub 2011/12/07. PubMed Central PMCID: PMC3251151. https://doi.org/10.1073/pnas.1111014108 PMID: 22143763

21. Heirbaut M, Strelkov SV, Weeks SD. Everything but the ACD, Functional Conservation of the Non-conserved Terminal Regions in sHSPs. In: Tanguay MR, Hightower EL, editors. The Big Book on Small Heat Shock Proteins. Cham: Springer International Publishing; 2015. p. 197–227.

22. Arrigo AP. Human small heat shock proteins: protein interactomes of homo- and hetero-oligomeric complexes: an update. FEBS Lett. 2013; 587(13):1959–69. Epub 2013/05/21. https://doi.org/10.1016/j.febslet.2013.05.011 PMID: 23684648

23. Haslbeck M, Weinkauf S, Buchner J. Regulation of the Chaperone Function of Small Hsps. In: Tanguay RM, Hightower LE, editors. The Big Book on Small Heat Shock Proteins. Heat Shock Proteins. 8: Springer International Publishing; 2015. p. 155–78.

24. Peschek J, Braun N, Rohrberg J, Back KC, Kriehuber T, Kastenmuller A, et al. Regulated structural transitions unleash the chaperone activity of alphaB-crystallin. Proc Natl Acad Sci U S A. 2013; 110(40):E3780–9. Epub 2013/09/18. PubMed Central PMCID: PMC3791731. https://doi.org/10.1073/pnas.1308898110 PMID: 24043785

25. Rogalla T, Ehrnsperger M, Preville X, Kotlyarov A, Lutsch G, Ducasse C, et al. Regulation of Hsp27 oligomerization, chaperone function, and protective activity against oxidative stress/tumor necrosis factor alpha by phosphorylation. J Biol Chem. 1999; 274(27):18947–56. Epub 1999/06/26. PMID: 10383393

26. Kato K, Hasegawa K, Goto S, Inaguma Y. Dissociation as a result of phosphorylation of an aggregated form of the small stress protein, hsp27. J Biol Chem. 1994; 269(15):11274–8. Epub 1994/04/15. PMID: 8157658

27. Ito H, Kamei K, Iwamoto I, Inaguma Y, Nohara D, Kato K. Phosphorylation-induced change of the oligomerization state of alpha B-crystallin. J Biol Chem. 2001; 276(7):5346–52. https://doi.org/10.1074/jbc.M009004200 PMID: 11096101

28. Lund AA, Rhoads DM, Lund AL, Cerny RL, Elthon TE. In vivo modifications of the maize mitochondrial small heat stress protein, HSP22. J Biol Chem. 2001; 276(32):29924–9. Epub 2001/06/09. https://doi.org/10.1074/jbc.M103373200 PMID: 11397800

29. Ficarro SB, McCleland ML, Stukenberg PT, Burke DJ, Ross MM, Shabanowitz J, et al. Phosphoproteome analysis by mass spectrometry and its application to Saccharomyces cerevisiae. Nat Biotechnol. 2002; 20(3):301–5. Epub 2002/03/05. https://doi.org/10.1038/nbt0302-301 PMID: 11875433

30. Gv Morrow, Tanguay R. Drosophila Small Heat Shock Proteins: An Update on Their Features and Functions. In: Tanguay RM, Hightower LE, editors. The Big Book on Small Heat Shock Proteins. Heat Shock Proteins. 8: Springer International Publishing; 2015. p. 579–606.

31. Zhai B, Villen J, Beausoleil SA, Mintseris J, Gygi SP. Phosphoproteome analysis of Drosophila melanogaster embryos. J Proteome Res. 2008; 7(4):1675–82. PubMed Central PMCID: PMC3063950. https://doi.org/10.1021/pr700696a PMID: 18327897

32. Bodenmiller B, Mueller LN, Pedrioli PG, Pflieger D, Junger MA, Eng JK, et al. An integrated chemical, mass spectrometric and computational strategy for (quantitative) phosphoproteomics: application to Drosophila melanogaster Kc167 cells. Mol Biosyst. 2007; 3(4):275–86. https://doi.org/10.1039/b617545g PMID: 17372656

33. Beaulieu JF, Arrigo AP, Tanguay RM. Interaction of Drosophila 27,000 Mr heat-shock protein with the nucleus of heat-shocked and ecdysone-stimulated culture cells. J Cell Sci. 1989; 92 (Pt 1):29–36. Epub 1989/01/01.

34. Michaud S, Lavoie S, Guimond MO, Tanguay RM. The nuclear localization of Drosophila Hsp27 is dependent on a monopartite arginine-rich NLS and is uncoupled from its association to nuclear speckles. Biochim Biophys Acta. 2008; 1783(6):1200–10. Epub 2008/03/15. https://doi.org/10.1016/j.bbamcr.2008.01.031 PMID: 18339325

35. Moutaoufik MT, Morrow G, Maaroufi H, Férard C, Finet S, Tanguay RM. Oligomerization and chaperone-like activity of Drosophila melanogaster small heat shock protein DmHsp27 and three arginine mutants in the alpha-crystallin domain. Cell Stress and Chaperones. 2016:1–12.

36. Michaud S, Morrow G, Marchand J, Tanguay RM. Drosophila small heat shock proteins: cell and organelle-specific chaperones? Prog Mol Subcell Biol. 2002; 28:79–101. Epub 2002/03/23. PMID: 11908067

37. Hayes D, Napoli V, Mazurkie A, Stafford WF, Graceffa P. Phosphorylation dependence of hsp27 multimeric size and molecular chaperone function. J Biol Chem. 2009; 284(28):18801–7. Epub 2009/05/05. PubMed Central PMCID: PMC2707219. https://doi.org/10.1074/jbc.M109.011353 PMID: 19411251

38. Ehrnsperger M, Graber S, Gaestel M, Buchner J. Binding of non-native protein to Hsp25 during heat shock creates a reservoir of folding intermediates for reactivation. EMBO J. 1997; 16(2):221–9. Epub 1997/01/15. PubMed Central PMCID: PMC1169629. https://doi.org/10.1093/emboj/16.2.221 PMID: 9029143

39. Shashidharamurthy R, Koteiche HA, Dong J, McHaourab HS. Mechanism of chaperone function in small heat shock proteins: dissociation of the HSP27 oligomer is required for recognition and binding of destabilized T4 lysozyme. J Biol Chem. 2005; 280(7):5281–9. Epub 2004/11/16. https://doi.org/10.1074/jbc.M407236200 PMID: 15542604

40. Marin R, Landry J, Tanguay RM. Tissue-specific posttranslational modification of the small heat shock protein HSP27 in Drosophila. Exp Cell Res. 1996; 223(1):1–8. Epub 1996/02/25. https://doi.org/10.1006/excr.1996.0052 PMID: 8635480

41. den Engelsman J, van de Schootbrugge C, Yong J, Pruijn GJ, Boelens WC. Pseudophosphorylated alphaB-Crystallin Is a Nuclear Chaperone Imported into the Nucleus with Help of the SMN Complex. PLoS One. 2013; 8(9):e73489. Epub 2013/09/12. PubMed Central PMCID: PMC3762725. https://doi.org/10.1371/journal.pone.0073489 PMID: 24023879

42. Beaulieu JF, Arrigo AP, Tanguay RM. Interaction of Drosophila 27000 Mr Heat-Shock Protein with the Nucleus of Heat-Shocked and Ecdysone-Stimulated Culture Cells. Journal of Cell Science. 1989; 92:29–36. PMID: 2777913

43. Haslbeck M, Peschek J, Buchner J, Weinkauf S. Structure and function of alpha-crystallins: Traversing from in vitro to in vivo. Biochim Biophys Acta. 2016; 1860(1 Pt B):149–66.

44. Theriault JR, Lambert H, Chavez-Zobel AT, Charest G, Lavigne P, Landry J. Essential role of the NH2-terminal WD/EPF motif in the phosphorylation-activated protective function of mammalian Hsp27. J Biol Chem. 2004; 279(22):23463–71. Epub 2004/03/23. https://doi.org/10.1074/jbc.M402325200 PMID: 15033973

45. Patel S, Vierling E, Tama F. Replica exchange molecular dynamics simulations provide insight into substrate recognition by small heat shock proteins. Biophys J. 2014; 106(12):2644–55. Epub 2014/06/19. PubMed Central PMCID: PMC4070073. https://doi.org/10.1016/j.bpj.2014.04.048 PMID: 24940782

46. Lee GJ, Roseman AM, Saibil HR, Vierling E. A small heat shock protein stably binds heat-denatured model substrates and can maintain a substrate in a folding-competent state. EMBO J. 1997; 16(3):659–71. Epub 1997/02/03. PubMed Central PMCID: PMC1169668. https://doi.org/10.1093/emboj/16.3.659 PMID: 9034347

47. Sharma KK, Kumar GS, Murphy AS, Kester K. Identification of 1,1'-bi(4-anilino)naphthalene-5,5'-disulfonic acid binding sequences in alpha-crystallin. J Biol Chem. 1998; 273(25):15474–8. Epub 1998/06/23. PMID: 9624133

48. Ghosh JG, Houck SA, Clark JI. Interactive domains in the molecular chaperone human alphaB crystallin modulate microtubule assembly and disassembly. PLoS One. 2007; 2(6):e498. Epub 2007/06/07. PubMed Central PMCID: PMC1876262. https://doi.org/10.1371/journal.pone.0000498 PMID: 17551579

49. Cheng G, Basha E, Wysocki VH, Vierling E. Insights into small heat shock protein and substrate structure during chaperone action derived from hydrogen/deuterium exchange and mass spectrometry. J Biol Chem. 2008; 283(39):26634–42. Epub 2008/07/16. PubMed Central PMCID: PMC2546550. https://doi.org/10.1074/jbc.M802946200 PMID: 18621732

50. Baranova EV, Weeks SD, Beelen S, Bukach OV, Gusev NB, Strelkov SV. Three-dimensional structure of alpha-crystallin domain dimers of human small heat shock proteins HSPB1 and HSPB6. J Mol Biol. 2011; 411(1):110–22. Epub 2011/06/07. https://doi.org/10.1016/j.jmb.2011.05.024 PMID: 21641913

51. Feil IK, Malfois M, Hendle J, van Der Zandt H, Svergun DI. A novel quaternary structure of the dimeric alpha-crystallin domain with chaperone-like activity. J Biol Chem. 2001; 276(15):12024–9. Epub 2001/ 03/30. https://doi.org/10.1074/jbc.M010856200 PMID: 11278766

52. Kundu M, Sen PC, Das KP. Structure, stability, and chaperone function of alphaA-crystallin: role of N-terminal region. Biopolymers. 2007; 86(3):177–92. https://doi.org/10.1002/bip.20716 PMID: 17345631

53. Laganowsky A, Benesch JL, Landau M, Ding L, Sawaya MR, Cascio D, et al. Crystal structures of truncated alphaA and alphaB crystallins reveal structural mechanisms of polydispersity important for eye lens function. Protein Sci. 2010; 19(5):1031–43. Epub 2010/05/05. PubMed Central PMCID: PMC2868245. https://doi.org/10.1002/pro.380 PMID: 20440841

54. Leroux MR, Melki R, Gordon B, Batelier G, Candido EP. Structure-function studies on small heat shock protein oligomeric assembly and interaction with unfolded polypeptides. J Biol Chem. 1997; 272 (39):24646–56. PMID: 9305934

55. Crack JA, Mansour M, Sun Y, MacRae TH. Functional analysis of a small heat shock/alpha-crystallin protein from Artemia franciscana. Oligomerization and thermotolerance. Eur J Biochem. 2002; 269 (3):933–42. PMID: 11846795

56. Sun Y, Mansour M, Crack JA, Gass GL, MacRae TH. Oligomerization, chaperone activity, and nuclear localization of p26, a small heat shock protein from Artemia franciscana. J Biol Chem. 2004; 279 (38):39999–40006. https://doi.org/10.1074/jbc.M406999200 PMID: 15258152

57. Crabbe MJ, Goode D. alpha-Crystallin: chaperoning and aggregation. Biochem J. 1994; 297 (Pt 3):653–4. PubMed Central PMCID: PMCPMC1137882.

58. Pasta SY, Raman B, Ramakrishna T, Rao Ch M. Role of the conserved SRLFDQFFG region of alpha-crystallin, a small heat shock protein. Effect on oligomeric size, subunit exchange, and chaperone-like activity. J Biol Chem. 2003; 278(51):51159–66. https://doi.org/10.1074/jbc.M307523200 PMID: 14532291

59. Kelley PB, Abraham EC. Thermally induced disintegration of the oligomeric structure of alphaB-crystallin mutant F28S is associated with diminished chaperone activity. Mol Cell Biochem. 2003; 252(1–2):273–8. PMID: 14577602

60. Horwitz J, Bova M, Huang QL, Ding L, Yaron O, Lowman S. Mutation of alpha B-crystallin: effects on chaperone-like activity. Int J Biol Macromol. 1998; 22(3–4):263–9. PMID: 9650081

61. Plater ML, Goode D, Crabbe MJ. Effects of site-directed mutations on the chaperone-like activity of alphaB-crystallin. J Biol Chem. 1996; 271(45):28558–66. PMID: 8910485

62. Capponi S, Geroldi A, Fossa P, Grandis M, Ciotti P, Gulli R, et al. HSPB1 and HSPB8 in inherited neuropathies: study of an Italian cohort of dHMN and CMT2 patients. J Peripher Nerv Syst. 2011; 16 (4):287–94. Epub 2011/12/20. https://doi.org/10.1111/j.1529-8027.2011.00361.x PMID: 22176143

63. Muranova LK, Weeks SD, Strelkov SV, Gusev NB. Characterization of Mutants of Human Small Heat Shock Protein HspB1 Carrying Replacements in the N-Terminal Domain and Associated with Hereditary Motor Neuron Diseases. PLoS One. 2015; 10(5):e0126248. PubMed Central PMCID: PMCPMC4429025. https://doi.org/10.1371/journal.pone.0126248 PMID: 25965061

64. Raman B, Ramakrishna T, Rao CM. Temperature dependent chaperone-like activity of alpha-crystallin. FEBS Lett. 1995; 365(2–3):133–6. PMID: 7781765

65. Datta SA, Rao CM. Differential temperature-dependent chaperone-like activity of alphaA- and alphaB-crystallin homoaggregates. J Biol Chem. 1999; 274(49):34773–8. PMID: 10574947

66. Delbecq SP, Klevit RE. One size does not fit all: the oligomeric states of alphaB crystallin. FEBS Lett. 2013; 587(8):1073–80. Epub 2013/01/24. https://doi.org/10.1016/j.febslet.2013.01.021 PMID: 23340341

67. Garrido C, Paul C, Seigneuric R, Kampinga HH. The small heat shock proteins family: the long forgotten chaperones. Int J Biochem Cell Biol. 2012; 44(10):1588–92. Epub 2012/03/28. https://doi.org/10.1016/j. biocel.2012.02.022 PMID: 22449631

68. McHaourab HS, Godar JA, Stewart PL. Structure and mechanism of protein stability sensors: chaperone activity of small heat shock proteins. Biochemistry. 2009; 48(18):3828–37. Epub 2009/03/28. PubMed Central PMCID: PMC2785012. https://doi.org/10.1021/bi900212j PMID: 19323523

69. Franzmann TM, Menhorn P, Walter S, Buchner J. Activation of the chaperone Hsp26 is controlled by the rearrangement of its thermosensor domain. Mol Cell. 2008; 29(2):207–16. Epub 2008/02/05. https://doi.org/10.1016/j.molcel.2007.11.025 PMID: 18243115

70. Basha E, Jones C, Wysocki V, Vierling E. Mechanistic differences between two conserved classes of small heat shock proteins found in the plant cytosol. J Biol Chem. 2010; 285(15):11489–97. Epub 2010/ 02/11. PubMed Central PMCID: PMC2857027. https://doi.org/10.1074/jbc.M109.074088 PMID: 20145254

71. Lelj-Garolla B, Mauk AG. Self-association and chaperone activity of Hsp27 are thermally activated. J Biol Chem. 2006; 281(12):8169–74. https://doi.org/10.1074/jbc.M512553200 PMID: 16436384

72. Chowdary TK, Raman B, Ramakrishna T, Rao CM. Mammalian Hsp22 is a heat-inducible small heat-shock protein with chaperone-like activity. Biochem J. 2004; 381(Pt 2):379–87. PubMed Central PMCID: PMCPMC1133843. https://doi.org/10.1042/BJ20031958 PMID: 15030316

73. Zhang K, Ezemaduka AN, Wang Z, Hu H, Shi X, Liu C, et al. A novel mechanism for small heat shock proteins to function as molecular chaperones. Sci Rep. 2015; 5:8811. PubMed Central PMCID: PMCPMC4351549. https://doi.org/10.1038/srep08811 PMID: 25744691

74. Das KP, Surewicz WK. Temperature-induced exposure of hydrophobic surfaces and its effect on the chaperone activity of alpha-crystallin. FEBS Lett. 1995; 369(2–3):321–5. PMID: 7649280

75. Smith JB, Liu Y, Smith DL. Identification of possible regions of chaperone activity in lens alpha-crystallin. Exp Eye Res. 1996; 63(1):125–8. PMID: 8983959

76. Weeks SD, Drinker M, Loll PJ. Ligation independent cloning vectors for expression of SUMO fusions. Protein Expr Purif. 2007; 53(1):40–50. PubMed Central PMCID: PMCPMC1892228. https://doi.org/10.1016/j.pep.2006.12.006 PMID: 17251035

77. Morrow G, Heikkila JJ, Tanguay RM. Differences in the chaperone-like activities of the four main small heat shock proteins of Drosophila melanogaster. Cell Stress Chaperones. 2006; 11(1):51–60. Epub 2006/04/01. PubMed Central PMCID: PMC1400613. https://doi.org/10.1379/CSC-166.1 PMID: 16572729

78. Moutaoufik MT, El Fatimy R, Nassour H, Gareau C, Lang J, Tanguay RM, et al. UVC-induced stress granules in mammalian cells. PLoS One. 2014; 9(11):e112742. PubMed Central PMCID: PMCPMC4237350. https://doi.org/10.1371/journal.pone.0112742 PMID: 25409157

79. Edgar RC. MUSCLE: multiple sequence alignment with high accuracy and high throughput. Nucleic Acids Res. 2004; 32(5):1792–7. Epub 2004/03/23. PubMed Central PMCID: PMC390337. https://doi.org/10.1093/nar/gkh340 PMID: 15034147